Published in final edited form as:
Nature. 2005 June 16; 435(7044): 911–915.

The nucleotide-dependent bending flexibility of tubulin regulates microtubule assembly

Hong-Wei Wang and **Eva Nogales**

Howard Hughes Medical Institute, UC Berkeley, Berkeley, CA 94720-3200 And Lawrence Berkeley National Laboratory

Abstract

The atomic structures of tubulin in a polymerized, straight protofilament, and in a curved conformation bound to a cellular depolymerizer are clearly distinct. Interestingly, the nucleotide content is identical, and in both cases the conformation of the GTP-containing intra-dimer interface is indistinguishable from the GDP-containing inter-dimer contact. Here we present two structures corresponding to the start and end points in the microtubule polymerization and hydrolysis cycles that illustrate the consequences of nucleotide state on longitudinal and lateral assembly. In the absence of depolymerizers GDP-bound tubulin shows distinctive intra- and inter-dimer interactions and thus distinguishes the GTP and GDP interfaces. A cold-stable GMPCPP polymer containing semi-conserved lateral interactions supports a model in which straightening of longitudinal interfaces happens sequentially, starting with a conformational change upon GTP binding that straightens the dimer enough for formation of lateral contacts into a non-tubular intermediate. Closure into a microtubule does not require GTP hydrolysis.

The dynamic behaviour of microtubules is key to their functions, and although is regulated by cellular factors during the cell cycle, it is an intrinsic property of the tubulin subunit[1,2,3]. The binding, hydrolysis, and exchange of nucleotide have been identified as central to the conformational flexibility that tubulin exhibits in its polymerization/depolymerization cycle. Structures of two different assembly states of tubulin are available at atomic resolution: tubulin in a polymerized, straight protofilament bound to the stabilizer taxol (obtained by electron crystallography of zinc-induced sheets[4,5]), which very closely corresponds to that of tubulin in microtubules[6]; and tubulin in a depolymerized, curved conformation bound to a fragment of the stathmin homologue RB3 and colchicine (obtained by X-ray crystallography)[7]. Interestingly, these clearly different structures have the same nucleotide content, in both cases the conformation of GTP-bound α-tubulin and of GDP-bound β-tubulin are the same, and intra- and inter-dimer contacts are practically indistinguishable. Here we present the structure GDP-bound tubulin in the absence of depolymerizing agents and show, for the first time, distinctive intra and inter dimer interactions. Still the question remained: how does the binding of GTP to the E-site affect the bending of the dimer, the dimer-dimer interface, and microtubule assembly? We have addressed this question by characterizing the assembly of tubulin bound to the non-hydrolysable GTP analogue GMPCPP into ribbon structures at low temperatures. We propose that these structures correspond closely to the open sheets visualized at the growing ends of microtubules[8].

Correspondence and requests for materials should be addressed to E.N. (e-mail: enogales@lbl.gov).

Supplementary Information accompanies the paper on *Nature*'s website (http://www.nature.com).

The authors have no financial interest concerning this work.

Structure of GDP-tubulin in the absence of depolymerizers

Divalent cations facilitate the self-assembly of GDP-tubulin into ring-like structures of curved protofilaments[9,10], and stabilize the protofilament peels observed at depolymerizing microtubule ends[11,12]. We found conditions in which closure does not happen and the protofilaments keep turning in a tight, one-start helix (Supplementary Information). The most common arrangement is a double-layered tube with 32 tubulin monomers in one turn of the outer layer and 24 in the inner layer (Fig S1a and Table S1). Cryo-EM images show diffraction up to 17-Å resolution (Fig. S1b and Fig S2). The double-layer character of the tubes results in systematic overlap of the Bessel terms (Fig S2) and makes it impossible to use traditional helical reconstruction[13]. We developed an iterative Fourier Bessel method by which the relative orientation of different tubes can be determined and used to produce a 3-D reconstruction[13]. We have implemented this methodology to obtain a reconstruction of GDP-tubulin at 12-Å resolution.

The averaged dataset of 19 images shows significant signal up to 10-Å resolution axially (Fig S1c; some averaged layer lines in Fig S3). Layer lines corresponding to the αβ dimer are noticeable, already indicating the presence of differences between monomers and dimers. The 3D-densities for the two layers were independently reconstructed using data up to 12-Å resolution (Fig 1a). Fourier shell correlation showed that the dimer densities from both layers are the same up to 15-Å (not shown) and thus that the GDP-tubulin dimer has basically the same conformation in the two layers, their different curvature arising from different inter dimer contacts.

In all the tubulin polymers characterized to date at medium to high resolution, zinc-sheets, microtubules and the RB3/colchicine-tubulin complex[5,6,7], α- and β-tubulin are very similar to each other and intra- and inter-dimer interfaces, which have different nucleotide content (the intra dimer interface contained a non-exchangeable GTP, while the inter dimer interface contained GDP at the exchangeable site (E-site)), are practically indistinguishable. It has been proposed that the conformation of GDP-bound tubulin in a microtubule lattice (or zinc-sheet) would be constrained as to resemble that when bound to GTP (the free energy for hydrolysis being stored in the microtubule lattice as mechanical constrain)[14,15,16]. On the other hand, the RB3/colchicine-bound structure could be affected by the binding of these ligands. In our structure of unconstrained, GDP-bound tubulin the intra- and inter-dimer interfaces are significantly different (Fig. 1a and Fig. S2 and S3). To compare the monomer structure and the subunit organization in our GDP-tubulin polymer with previous studies we docked the atomic models of tubulin into our reconstructions (Fig 1b). The overall fit of the monomer is good, but there is extra density at the C-terminus of both subunits in both layers that corresponds to the C-terminal amino acids disordered in the crystals but contributing significantly to our 12-Å reconstruction. In addition, a distinctive conformational change occurs, as the interfaces open but the interaction between H10 in one monomer and H6 in the other is maintained. Although the conformation of our monomers is not exactly either of the existing crystal structures, docking was slightly optimized when we used the β-tubulin structure from the RB3-bound model[7] and the α-tubulin structure from the electron crystallography study[5], suggesting two distinct monomer conformations.

The extent and direction of bending between tubulin monomers in this GDP state is similar but yet distinctive from that seen in the structure of the tubulin-RB3-colchicine complex (Fig. 2; Fig. S4). The bending at the intra-dimer interface is smaller and more tangential. The inter- and intra-dimer contacts are practically indistinguishable in RB3-tubulin, while in our structure, the direction of inter-dimer bending is the same as in RB3-tubulin (thus slightly different from that within its dimer), but of significantly larger magnitude, which varies between the inner and outer layer. The small rearrangement seen at the intra-dimer interface

in the RB3-tubulin structure may be due to the presence of colchicine at the site[17]. On the other hand, it is possible that the inter-dimer interface gets locked into an "intra-dimer-like" state by way of the RB3 alpha helix that runs along the surface of both dimers[7]. Our study indicates that, irrespective of whether bound or unbound by a depolymerizer, the bending of the intra- and inter-dimer interfaces in unconstrained, GDP-bound tubulin is incompatible with the formation of the canonical lateral contacts in microtubules. While this explains why GDP-bound dimers or oligomers cannot be incorporated into the microtubule, it leaves open the question of how binding of GTP would result in the "straightening" of protofilaments observed in microtubules.

Structure of GMPCPP ribbons and tubes formed at low temperatures

The presence of GTP at the E-site would need to have an effect, both at the inter-dimer interface where it resides, and at the intra-dimer interface, 40 Å apart, in order to straighten monomer contacts. One possibility is that binding of GTP straightens the dimer and inter-dimer contacts to a point where lateral contacts as those in microtubules can form, and that further straightening occurs upon closure of the polymer into a cylinder. This idea is suggested by cryo-EM images of microtubules with open, curved sheets at their growing ends[8] that have been modelled to mechanically straighten as the microtubule closes[18]. The sheets are more often seen in conditions of fast growth, and it is not known whether hydrolysis occurs before sheet closure.

In order to visualize the curvature, structure, and self-association of GTP-containing protofilaments we have studied the self-assembly of tubulin in the presence of the non-hydrolysable analogue GMPCPP. Previous studies showed that microtubules made of GMPCPP-bound tubulin have a slightly different axial repeat[19], and when depolymerized by calcium breakdown into curved protofilaments with dramatically less curvature than those of GDP-containing microtubules[20]. These results supported a model in which GTP hydrolysis increased the curvature of protofilaments, but the irregular nature of the peeled protofilaments precluded their characterization. Here we found that at low temperatures GMPCPP-bound tubulin forms helical ribbons reminiscent of the structures seen following depolymerization of GMPCPP microtubules[20]. The ribbons contain a few protofilaments early in the incubation process, but grow to more than 20 protofilaments that close into a tube of about 500-Å diameter (Fig. S5). Diffraction patterns from both small, open ribbons and larger, closed tubes show the same tubulin arrangement: head-to-tail association into protofilaments that interact laterally with the same stagger as in microtubules (Fig. S6). We used cryo-EM and helical reconstruction to obtain a structure at 18-Å resolution of this GMPCPP state of tubulin (Fig. 3a). The structure (as predicted from the diffraction of ribbons and tubes) shows the presence of protofilament pairs (Fig. 3a and S7). Docking of β-tubulin from zinc-sheets shows that the atomic model fits extremely well within our density (Fig. 3b). At this resolution α and β subunits are impossible to tell apart and the intra- and inter-dimer contacts indistinguishable (notice that in this case both are in the same nucleotide state!). The protofilaments are curved approximately radially, with the inside of our tubes corresponding to the outside of the microtubule. The radial bend between subunits is about 5° (Fig. 4a), significantly smaller than the intra dimer bend of 12° in our GDP-bound structure. Thus, both interfaces straighten upon GTP (GMPCPP) binding.

We found that the lateral interactions between the two protofilaments in one pair are indistinguishable from those seen in microtubules, while the contacts between pairs use regions of tubulin that in microtubules define the external grooves between protofilaments (Fig. 4a). Thus, the alternate contacts have "rolled out" by about 20 Å (~60° rotation). Given this alternation of lateral interfaces it is remarkable that the lateral stagger is conserved (there is no longitudinal "slippage"), suggesting that this organization of tubulin is related to the microtubule assembly process. This idea was supported by the direct conversion of ribbons into microtubules when temperature was increased to 37 °C (Fig. 4b, c). Closure into a

microtubule requires the "rolling back" of the alternate lateral contact and results in the straightening of protofilaments.

Our interpretation is that the GMPCPP ribbon structures are likely to correspond structurally to the curved ends of open sheets at the ends of growing microtubules[8]. At higher temperatures closure into microtubules follows very closely the formation of the sheets; they are seen when subunits addition is significantly faster than hydrolysis, as in conditions of fast net polymerization[8]. If GTP-tubulin self-associates at low temperatures, when closure is delayed or precluded, it rapidly hydrolyzes GTP upon formation of longitudinal interactions, and then curves into the GDP state. When hydrolysis is precluded by using a non-hydrolysable analogue, the straighter conformation is maintained and sheets (ribbons) grow that are able to close when the temperature is risen.

Structural Pathway in the GTP-driven Assembly of Microtubules

The present study shows that the GDP state of tubulin results in longitudinal self-association with two distinct kinks at the intra, GTP-containing interface and the inter, GDP-containing contact, the latter kink being more flexible and larger in magnitude. This strongly suggests that binding of GTP at the E-site will have an effect on the structure of tubulin resulting in the formation of smaller and better-defined kinks between interacting dimers. Supporting experimental evidence comes from the visualization of peeling ends of calcium-depolymerized GMPCPP microtubules[20] and from this structural work. The small tangential bend within the GDP-bound dimer may not be sufficient to inhibit binding to a growing microtubule end (major regions in lateral contacts are flexible loops that could accommodate a slightly different geometry). But the bend between GDP-tubulin dimers seems too large to allow for lateral contacts formation, in agreement with the fact that GDP-bound tubulin cannot incorporate into microtubules. We propose that the binding of GTP at the E-side is likely to have three effects: 1) to reduce the dimer-dimer bending by locally changing the conformation around the nucleotide at the interface; 2) likely to straighten the dimer, a long range allosteric change that could involve helix H7 and the following T7 loop in β-tubulin, which link the intra- and inter-dimer interfaces; and 3) to fine tune the conformation of the monomer so as to strengthen lateral contacts. These three changes, or a subset of them, allow for the partial straightening of protofilaments that are able to form lateral contacts otherwise inhibited in the more curved GDP state. Lateral association of tubulin into curved sheets would be followed by a distinct, final straightening process that will close the surface of the microtubule. Our study supports separation of the straightening process into two stages. Most importantly, it provides a pseudo-atomic model of this sheet that illustrates a bimodal mechanism of lateral protofilament interaction preceding microtubule closure. Finally, our study proves that sheet closure does not require GTP hydrolysis.

Supplementary Material

Refer to Web version on PubMed Central for supplementary material.

Acknowledgements

We thank Georjana Barnes for fluorescent tubulin and Stefan Westermann for help with the optical microscopy. We thank Ken Downing, Patricia Grob, and Andres Leschziner for their comments on the manuscript. We are thankful to Willy Wriggers for generating the energy minimized atomic models after addition of missing loops. This work was funded by a grant from NIHGMS to E.N. and by the Office of Biological and Environmental Research of the U.S. Department of Energy. E.N. is a Howard Hughes Medical Investigator.

References

1. Desai A, Mitchison TJ. Microtubule polymerization dynamics. Annu Rev Cell Dev Biol 1997;13:83–117. [PubMed: 9442869]
2. Jordan MA. Mechanism of action of antitumor drugs that interact with microtubules and tubulin. Curr Med Chem Anti-Canc Agents 2002;2:1–17.
3. Heald R, Nogales E. Microtubule dynamics. J Cell Sci 2002;115:3–4. [PubMed: 11801717]
4. Nogales E, Wolf SG, Downing KH. Structure of the αβ tubulin dimer by electron crystallography. Nature 1998;391:199–203. [PubMed: 9428769]
5. Löwe J, Li H, Downing KH, Nogales E. Refined structure of αβ-tubulin at 3.5 Å resolution. J Mol Biol 2001;313:1045–1057. [PubMed: 11700061]
6. Li H, DeRosier DJ, Nicholson WV, Nogales E, Downing KH. Microtubule Sructure at 8 Å resolution. Structure 2002;10:1317–1328. [PubMed: 12377118]
7. Ravelli RB, Gigant B, Curmi PA, Jourdain I, Lachkar S, Sobel A, Knossow M. Insight into tubulin regulation from a complex with colchicines and a stathmin-like domain. Nature 2004;428:198–202. [PubMed: 15014504]
8. Chrétien D, Fuller SD, Karsenti E. Structure of growing microtubule ends: two-dimensional sheets close into tubes at variable rates. J Cell Biol 1995;129:1311–1328. [PubMed: 7775577]
9. Howard WD, Timasheff SN. GDP state of tubulin: stabilization of double rings. Biochemistry 1986;25:8292–8300. [PubMed: 3814585]
10. Nicholson WV, Lee M, Downing KH, Nogales E. Cryo-electron microscopy of GDP-tubulin rings. Cell Biochem Biophys 1999;31:175–183. [PubMed: 10593258]
11. Mandelkow EM, Mandelkow E, Milligan RA. Microtubule dynamics and microtubule caps: A time-resolved cryo-electron microscopy study. J Cell Biol 1991;114:977–991. [PubMed: 1874792]
12. Tran PT, Joshi P, Salmon ED. How tubulin subunits are lost from the shortening ends of microtubules. J Struct Biol 1997;118:107–118. [PubMed: 9126637]
13. Wang H-W, Nogales E. An iterative Fourier–Bessel algorithm for reconstruction of helical structures with severe Bessel overlap. J. Struct. Biol 2005;149:65–78. [PubMed: 15629658]
14. Caplow M, Ruhlen RL, Shanks J. The free energy for hydrolysis of a microtubule-bound nucleotide triphosphate is nearly zero: all of the free energy for hydrolysis is stored in the microtubule lattice. J Cell Biol 1994;127:779–788. [PubMed: 7962059]
15. Mickey B, Howard J. Rigidity of microtubules is increased by stabilizing agents. J Cell Biol 1995;130:909–917. [PubMed: 7642706]
16. Hyman AA, Karsenti E. Morphogenetic Properties of Microtubules and Mitotic Spindle Assembly. Cell 1996;84:401–410. [PubMed: 8608594]
17. Andreu JM, Gorbunoff MJ, Medrano FJ, Timasheff SN. Mechanism of colchicine binding to tubulin. Tolerance of constituents in ring C' of biphenyl analogues. Biochemistry 1991;30:3777–3786. [PubMed: 2015233]
18. Jánosi IM, Chrétien D, Flyvbjerg H. Modeling elastic properties of microtubule tips and walls. Eur Biophys J 1998;27:501–513. [PubMed: 9760731]
19. Hyman AA, Chrétien D, Severin F, Wade RH. Structural changes accompanying GTP hydrolysis in microtubules: information from a slowly hydrolyzable analogue guanylyl-(α, β)-methylenediphosphonate. J Cell Biol 1995;128:117–125. [PubMed: 7822409]
20. Müller-Reichert T, Chrétien D, Severin F, Hyman AA. Structural changes at microtubule ends accompanying GTP hydrolysis: information from a slowly hydrolyzable analogue of GTP, guanylyl (α, β)methylenediphosphonate. PNAS 1998;95:3661–3666. [PubMed: 9520422]

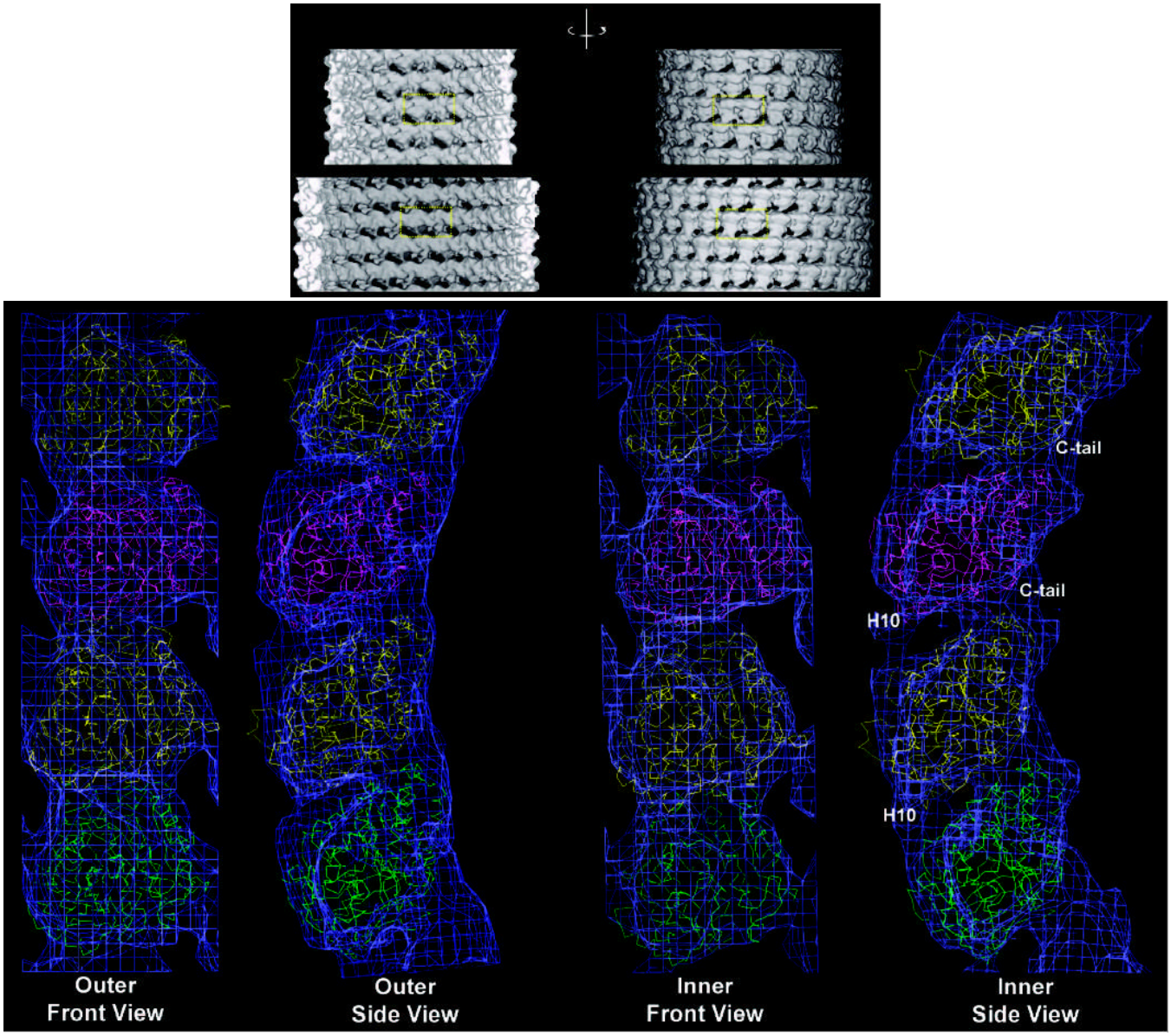

Fig. 1. Cryo-EM reconstruction of double-layered tubes of GDP-bound tubulin and docking of crystallographic models

(a) 3-D densities for the inner (top) and outer (bottom) layers of the GDP-tubulin tubes. Inside view of the tubes on the left, outside view on the right. Dimer boundaries are indicated by yellow boxes. (b) The crystallographic structures of tubulin were manually docked into the cryo-EM densities of the outer and inner layers of the tubes. β-tubulins (1SA0) are shown in yellow, α-tubulins (1JFF) are shown in green for the lower dimer and in magenta for the top dimer. Major regions of discrepancy with the crystal structures are indicated in the last panel.

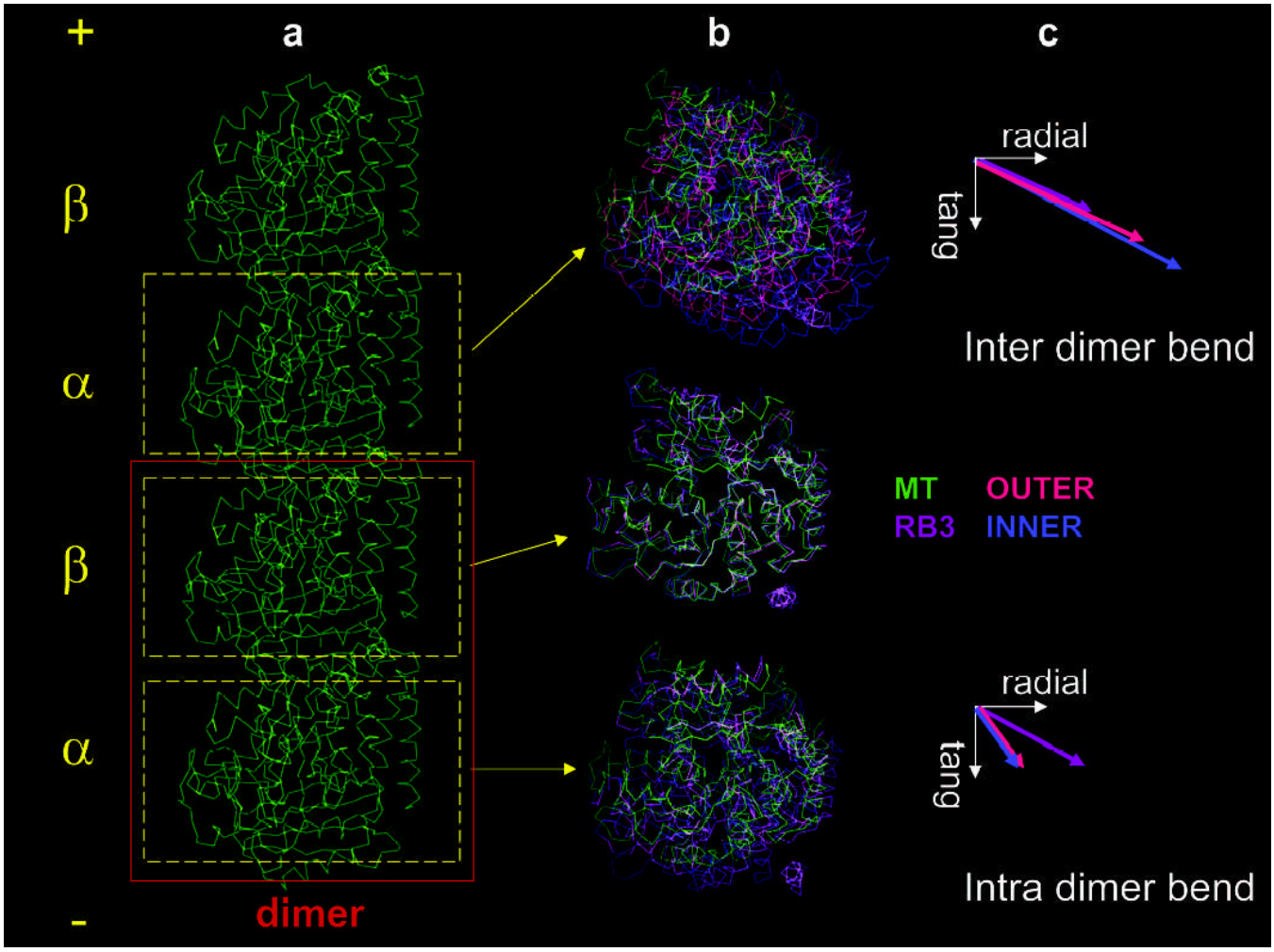

Fig. 2. Intra- and inter-dimer bends in different tubulin polymers

(a) Two dimers in a microtubule (plus-end at the top). The red box marks the lower dimer. The dashed yellow boxes indicate the monomers shown in the end-on views in (b). (b) The microtubule (green), RB3-bound structure (violet), outer (orange-red) and inner layer of the GDP tubes (blue) were aligned on the first β subunit. The bottom superposition shows the displacements due to the intra-dimer bending, and the top shows the displacements due to the inter-dimer bending. (c) Relative magnitude (arrow length) and the radial and tangential components of each bend.

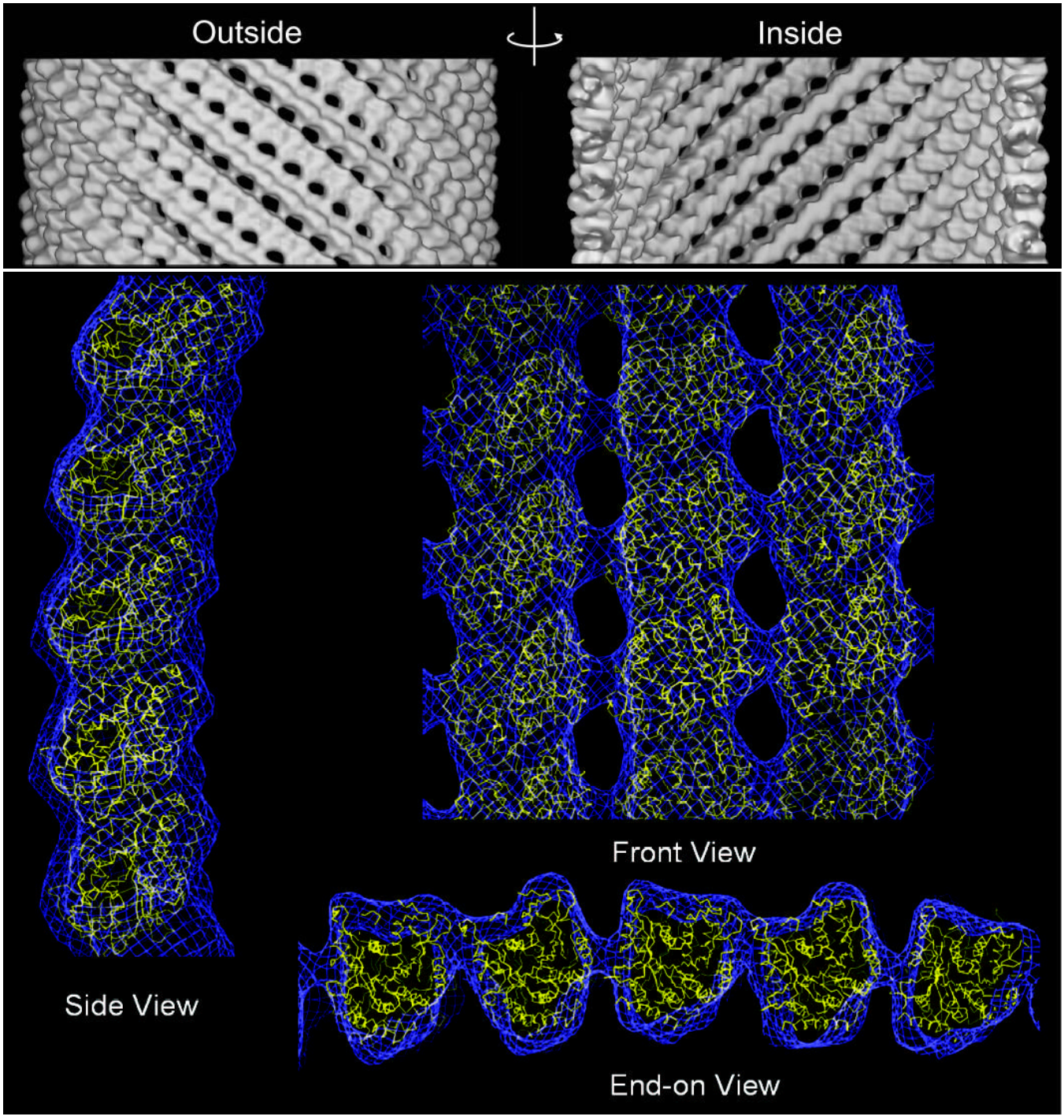

FIG. 3. Cryo-EM reconstruction of GMPCPP-tubulin tubes and docking of the crystallographic model

(a) 3-D densities of the GMPCPP tubulin tubes. Notice the association of protofilaments in pairs. (b) β-tubulin (1JFF) was manually docked into the density of the GMPCPP tube. The small outward curvature of the protofilaments is clearly seen in the Side View on the left (right surface corresponds to the outside of the microtubule). The Front View shows the lateral stagger between protofilaments, identical to that in microtubules. The End-on View shows more clearly the pairing of protofilaments. Within a pair the lateral contacts are indistinguishable from those

in microtubules, but the lateral contact between pairs has been displaced towards the inside surface of the tube.

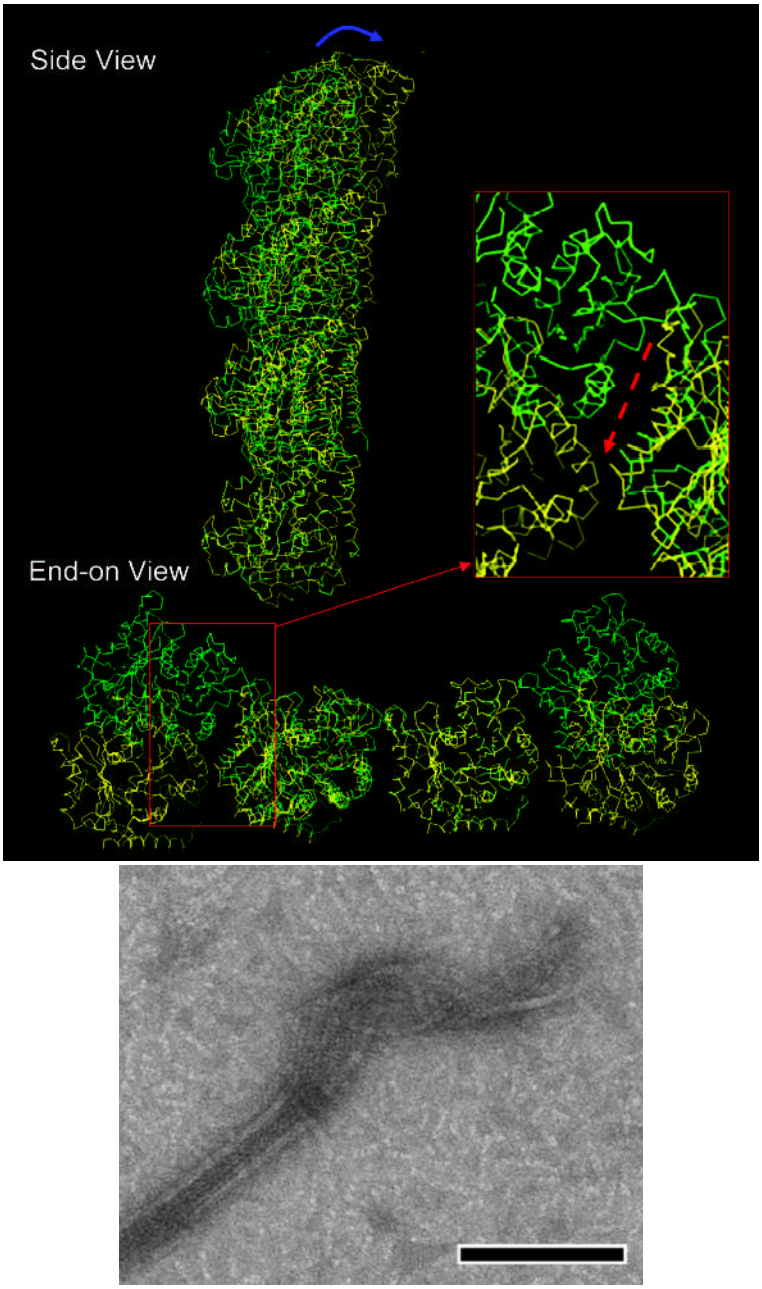

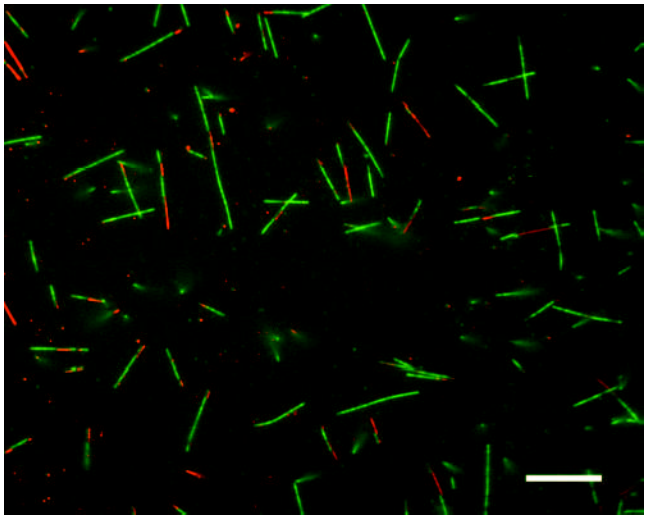

Fig. 4. GMPCPP tubes: comparison with and conversion into microtubules

(a) GMPCPP tube (yellow) and microtubule (green): Side View illustrating radial bending (blue arrow); End-on View showing how the lateral contact that results in the closure of microtubules is maintained within a protofilament pair, but is displaced between pairs (red arrow on inset). (b) Direct conversion of GMPCPP tubes into microtubules at 37 °C visualized by negative-stain electron microscopy (scale bar 100 nm). (c) Fluorescence microscopy of microtubules formed by mixing two populations of differentially labelled GMPCPP tubes before warming the solution, proving that conversion does not involve a depolymerization step (scale bar 10 μm).